RSC Advances

PAPER

View Article Online
View Journal | View Issue

Published on 04 August 2014. Downloaded by The University of Melbourne Libraries on 11/10/2014 09:08:59.

Cite this: *RSC Adv.*, 2014, **4**, 37556

Modification of tungsten trioxide with ionic liquid for enhanced photocatalytic performance

Jingjing Liu, Suiqi Han, Jia Li and Jun Lin*

Received 9th July 2014
Accepted 4th August 2014

DOI: 10.1039/c4ra06848c

www.rsc.org/advances

To develop WO_3, a narrow band gap semiconductor with a deep valence band, into an efficient visible light photocatalyst, we modified WO_3 with an ionic liquid [Bmim]I through a facile impregnation method in this study. Upon visible light irradiation, the [Bmim]I-modified WO_3 has been shown to have significantly higher photocatalytic activity than its unmodified counterparts for the degradation of RhB in aqueous solution. The effects of ionic liquid modification on the physicochemical properties of WO_3 and its enhanced photocatalysis were investigated in detail using various characterization methods and analysis of photogenerated hydroxyl radicals. It was revealed that the ionic liquid is bound to the surface of WO_3 after the modification. The presence of a surface-bound imidazolium ring was demonstrated to effectively suppress the recombination of photoexcited electron–hole pairs, resulting in enhanced photocatalysis compared to [Bmim]I-modified WO_3. Furthermore, the [Bmim]I-modified WO_3 exhibited sufficient stability and recyclability with respect to photocatalytic activity, which could make it a promising photocatalyst for practical applications.

1. Introduction

For complete utilization of solar light, the development of narrow band gap semiconductors as efficient visible light photocatalytic materials has become a widely researched topic in photocatalysis in recent years.[1–3] Among various narrow band gap semiconductors, tungsten trioxide (WO_3) with a band gap of 2.6–2.8 eV has been attracting considerable attention because of its stable physicochemical properties, non-toxicity, resistance to photocorrosion, and especially the strong oxidation ability of the holes photogenerated in the valence band (+3.1–3.2 V *vs.* NHE).[4–8] However, because of the low conduction band edge of WO_3 (+0.3–0.5 V *vs.* NHE), the electrons photoexcited in the conduction band cannot be efficiently consumed by oxygen molecules through a one-electron reduction process ($E^o(O_2/O_2^{-\bullet}) = -0.33$ V *vs.* NHE), which results in fast charge recombination and poor photocatalytic performance. This small charge separation in WO_3 is a serious drawback in the development of WO_3 as an efficient visible light photocatalyst. Recently, considerable efforts have been undertaken to improve the photocatalytic performance of WO_3 for the degradation of organic pollutants and for O_2 evolution. Typically, Pt-loaded WO_3 is reported to exhibit high photocatalytic activity under visible light irradiation because the surface Pt promotes the multi-electron reduction of the adsorbed oxygen ($E^o(O_2/H_2O_2) =$ +0.695 V *vs.* NHE and $E^o(O_2/2H_2O) =$ +1.229 V *vs.* NHE), resulting in charge separation.[9,10] Subsequently, several studies have been carried out on the morphology control of Pt/WO_3 and the surface modification of WO_3 with Pd, Pt/Au, CuO, Cu(II) clusters or graphene.[11–16] Meanwhile, nanostructured WO_3 with controlled morphologies or microstructures was also demonstrated to have an enhanced photocatalytic activity due to its large surface area and novel structure.[7,17] These studies have made significant contributions to the improvement of the photocatalytic performance of the narrow band gap semiconductor WO_3.

Ionic liquids (IL), a new class of reaction media and solvents, have been extensively employed in organic synthesis, catalysis, separation, and CO_2 capture because of their unique characteristics such as thermal stability, negligible vapor pressure, high ionic conductivity, good dissolving ability, environmentally friendly features, and wide electrochemical windows.[18,19] The development of ionic liquids as green reaction media has also provided numerous new opportunities for the synthesis and performance optimization of inorganic materials.[20] Recently, it was reported that the visible light photocatalytic activities of semiconductors, such as TiO_2 and BiOI, can be improved by the surface modification of ionic liquids.[21,22] To develop WO_3, a narrow band gap semiconductor with a deep valence band, as an efficient visible light photocatalyst, we modified WO_3 with an ionic liquid of [Bmim]I (1-butyl-3-methylimidazolium iodide) using a facile impregnation method in water at 80 °C in this study. The [Bmim]I-modified WO_3 samples were demonstrated to have significantly higher photocatalytic activity compared to bare WO_3. The effects of the ionic liquid on the physicochemical properties of WO_3 and the

Department of Chemistry, Renmin University of China, Beijing 100872, People's Republic of China. E-mail: jlin@chem.ruc.edu.cn; Fax: +86-10-62516444; Tel: +86-10-62514133

This journal is © The Royal Society of Chemistry 2014

Published on 04 August 2014. Downloaded by The University of Melbourne Libraries on 11/10/2014 09:08:59.

enhanced photocatalysis were examined in detail based on various characterization methods and the analysis of photogenerated ˙OH radicals in the presence and absence of soluble oxygen. To our knowledge, this is the first report of utilizing an ionic liquid modification for improving the photocatalytic activity of a narrow band gap semiconductor with a deep valence band.

2. Experimental

2.1. Reagents

The chemicals that were used as received in this work included: tungsten trioxide (WO_3, 99.8%, Alfa Aesar), 1-butyl-3-methylimidazolium iodide ([Bmim]I, 99%, Lanzhou Greenchem. ILs, LICP, CAS), *tert*-butyl alcohol (TBA, AR 99%, Alfa Aesar), rhodamine B (RhB, 99%, Acros), triethanolamine (TEOA, AR 98%, Sinopharm Chemical Reagent Beijing Co., Ltd.), terephthalic acid (AR, 98.5%, Sinopharm Chemical Reagent Beijing Co., Ltd.), and NaOH (AR, 96%, Sinopharm Chemical Reagent Beijing Co., Ltd.). Deionized water was used throughout the experiments. For clear identification, the structure of the ionic liquid [Bmim]I is shown in Scheme 1.

2.2. Preparation of [Bmim]I-modified WO_3

The modification of WO_3 with [Bmim]I was carried out using a facile impregnation method in water at 80 °C. In detail, the desired amount of [Bmim]I was slowly added to 200 mL aqueous solution of NaOH (5 mM). The mixture was stirred at 80 °C for 0.5 h to prepare an optically transparent solution. Subsequently, 1.1593 g of WO_3 was added to the abovementioned solution. The molar ratios of [Bmim]I to WO_3 (R_{IL}) in the suspensions were 0.0, 1.2, 1.5, and 1.7. The resulting suspensions were then stirred at 80 °C for 4 h before being naturally cooled to room temperature. The resulting precipitates were collected by centrifugation and washed thoroughly with deionized water and ethanol. Finally, the samples were dried at 80 °C to form bare WO_3 ($R_{IL} = 0$) and [Bmim]I-modified WO_3 (denoted as IL-WO_3) with different R_{IL} values.

2.3. Characterization

X-ray diffraction (XRD) patterns of the as-prepared samples were recorded on an X-ray diffractometer (Shimadzu, XRD-7000) using Cu Kα as X-ray radiation ($\lambda = 1.5418$ Å). The accelerating voltage and applied current were 40 kV and 30 mA, respectively. The morphologies were observed with a field-emission scanning electron microscope (FESEM) (JEOL, JSM-7401E). The UV-vis diffuse reflectance spectra of the samples were obtained using a spectrophotometer (Hitachi, U-3900) equipped with a diffuse reflectance accessory, and $BaSO_4$ was used as the reference. The FT-IR spectra were collected with an IRPrestige-21 FT-IR spectrophotometer. X-ray photoelectron spectroscopy (XPS) measurements were conducted on an ESCALAB 250Xi spectrometer with Al Kα radiation. All the binding energies were referenced to the C1s peak (284.6 eV) of the surface adventitious carbon.

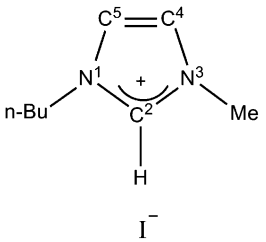

Scheme 1 Structure of 1-butyl-3-methylimidazolium iodide ([Bmim]I).

2.4. Photocatalytic activity experiments

The photocatalytic activities of the as-prepared samples were evaluated by observing the degradation of RhB in an aqueous solution. A total of 0.01 g of the catalyst was suspended in 100 mL of aqueous RhB solution ($\sim 10^{-5}$ M). A 300 W Xe arc lamp (CHFXM150, Beijing Trusttech. Co. Ltd.) equipped with a wavelength cutoff filter for $\lambda > 420$ nm was used as the light source and positioned approximately 8 cm above the aqueous suspension. Prior to irradiation, the suspension was magnetically stirred for an hour in the dark to ensure the establishment of equilibrium between the catalyst surface and RhB molecules. At a given irradiation time interval of 30 min, 5 mL of the suspension was sampled, and then the catalyst and RhB solution were separated by centrifugation. The concentration of RhB was determined by monitoring the change in the absorption spectrum of absorbance at 554 nm with a Hitachi U-3310 spectrophotometer.

In general, triethanolamine (TEOA) can act as an effective hole scavenger in photocatalytic reactions, while *tert*-butyl alcohol (TBA) is an ˙OH scavenger since its reaction with ˙OH radicals has a high rate constant ($k = 6 \times 10^8$).[23] To investigate the roles of the holes and the ˙OH radical in the photocatalytic degradation of RhB over these catalysts, the degradation of RhB over these catalysts irradiated with the abovementioned light source was also evaluated in the presence of TEOA (10 mM) or TBA (10 mM) in the same manner.

2.5. Analysis of photogenerated ˙OH radicals

The photogeneration of the ˙OH radicals over the photo-irradiated suspensions of bare WO_3 and IL-WO_3 ($R_{IL} = 1.5$) in the presence or absence of soluble oxygen was measured by a fluorescence technique using terephthalic acid as a chemical trap of ˙OH radicals.[24] Terephthalic acid readily reacts with ˙OH to only form 2-hydroxyterephthalic acid (reaction 1), a significantly fluorescent product. The experimental procedure was similar to the photocatalytic activity measurements described above. Briefly, the catalyst powder was suspended in an aqueous solution of terephthalic acid (0.5 mM) and NaOH (2.0 mM). Prior to irradiation, the suspension was magnetically stirred in a cuvette for an hour in the dark to ensure the establishment of the equilibrium between the catalyst surface and terephthalic acid. At given irradiation time intervals, 5 mL of the suspension was collected and filtered for fluorescence spectral measurements. The fluorescence emission intensity of 2-hydroxyterephthalic acid was detected at 425 nm with excitation at 315 nm

Published on 04 August 2014. Downloaded by The University of Melbourne Libraries on 11/10/2014 09:08:59.

using a spectrofluorometer (PerkinElmer LS55). In the case of measurement in the absence of soluble oxygen, the suspension was magnetically stirred in a cuvette and continuously bubbled with nitrogen gas for an hour in the dark, and subsequently sealed with a cap before irradiation.

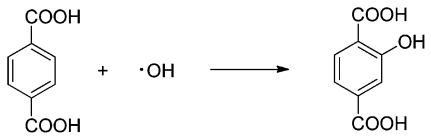

(1)

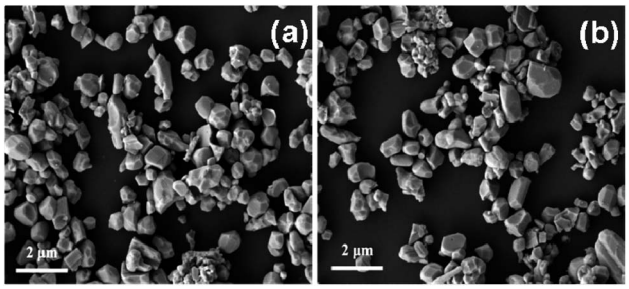

Fig. 2 FESEM images of bare WO_3 (a) and IL-WO_3 (R_{IL} = 1.5) (b).

3. Results and discussion

3.1. Physicochemical properties

The XRD patterns of the bare WO_3 and IL-WO_3 with different R_{IL} values are displayed in Fig. 1. All the samples exhibit a single monoclinic phase of well-crystallized WO_3 according to the JCPDS file (no. 43-1035). No other phases and changes in the full widths at half-maximum (FWHM) were observed after the [Bmim]I modification, as is expected on the basis of the mild conditions of the modification procedure. The results suggest that the ionic liquid modification occurs on the surface rather than inside the bulk WO_3, and does not affect the phase structure and crystallinity of WO_3. The FESEM observations (Fig. 2) show that both the bare WO_3 and IL-WO_3 (R_{IL} = 1.5) consist of dispersed large and fine particles with irregular polyhedral shapes. The sizes of the large and fine particles are approximately 0.5–1 μm and 100–300 nm, respectively. No apparent changes in the morphology and size distribution of the particles were observed after the ionic liquid modification.

The FT-IR spectra of the bare WO_3, IL-WO_3 (R_{IL} = 1.5) and [Bmim]I further demonstrate the presence of [Bmim]I on the surface of WO_3 (Fig. 3). In the FT-IR spectra of the bare WO_3 and IL-WO_3, the bands corresponding to the stretching vibrations of W=O and W–O bonds in WO_3 are clearly observed below 1000 cm^{-1}.[25,26] A broad band centered at 3450 cm^{-1} is associated with the stretching vibrations of hydrogen-bonded surface water molecules and hydroxyl groups.[2] It should be noted that several bands appear in the spectra of IL-WO_3 and [Bmim]I but are absent in that of the bare WO_3. Among these bands, the characteristic bands of the imidazolium ring at approximately 3142 cm^{-1} correspond to the symmetric and asymmetric stretches of the HCCH bonds in positions four and five of the imidazolium ring.[27] Two other bands at 2859 and 2926 cm^{-1} belong to the alkyl chain.[28] The sharp peaks at 1580 and 1170 cm^{-1} are consistent with the in-plane deformation vibrations of the imidazolium skeleton atoms and C–H bonds, respectively.[28] Furthermore, a new band near 535 cm^{-1} was observed for IL-WO_3 only, which may be due to the formation of W–O–C bonds caused by the surface modification of [Bmim]I.

The surface elemental compositions and chemical states of the bare WO_3 and IL-WO_3 (R_{IL} = 1.5) were studied by X-ray photoelectron spectroscopy (XPS). The XPS survey spectra (Fig. 4a) reveal the existence of W, O, and C in both the samples. Fig. 4b displays the XPS spectra of W4f core levels in both the samples. It can be observed that two peaks for the W4f of the bare WO_3 are located at the binding energies of 35.6 and 37.8 eV, attributed to $W4f_{7/2}$ and $W4f_{5/2}$, respectively, which are in good agreement with those of tungsten(VI) trioxide.[29–31] Note that the doublet is found to visibly shift toward a lower binding energy after the [Bmim]I modification in the case of IL-WO_3 (R_{IL} = 1.5). This observed shift in binding energy suggests an interaction between the surface W^{6+} and $[Bmim]^+$ adsorbed on the WO_3. As shown in Fig. 4c, there are two oxygen species in both the samples. The dominant peak located at approximately 530.3 eV is characteristic of the lattice oxygen (O_L) in WO_3,[32,33] while the other peak at 531.3 eV could be mainly attributed to the surface oxygen (O_S) present as hydroxyl groups on the

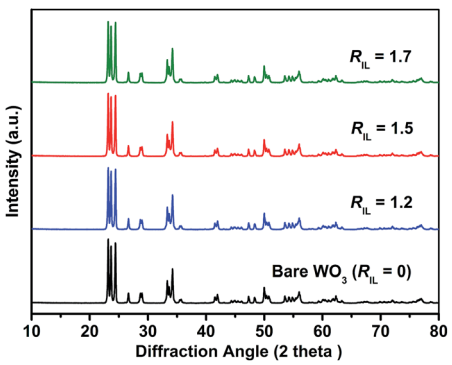

Fig. 1 X-ray diffraction patterns of bare WO_3 and IL-WO_3 with different R_{IL} values.

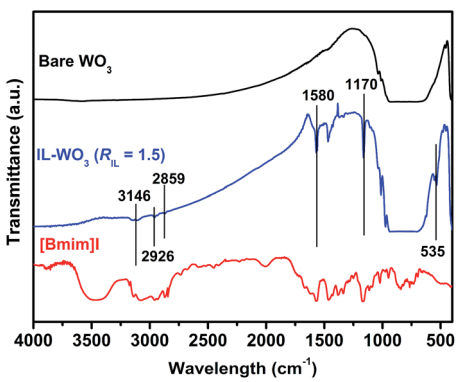

Fig. 3 FT-IR spectra of bare WO_3, IL-WO_3 (R_{IL} = 1.5) and [Bmim]I.

This journal is © The Royal Society of Chemistry 2014

Published on 04 August 2014. Downloaded by The University of Melbourne Libraries on 11/10/2014 09:08:59.

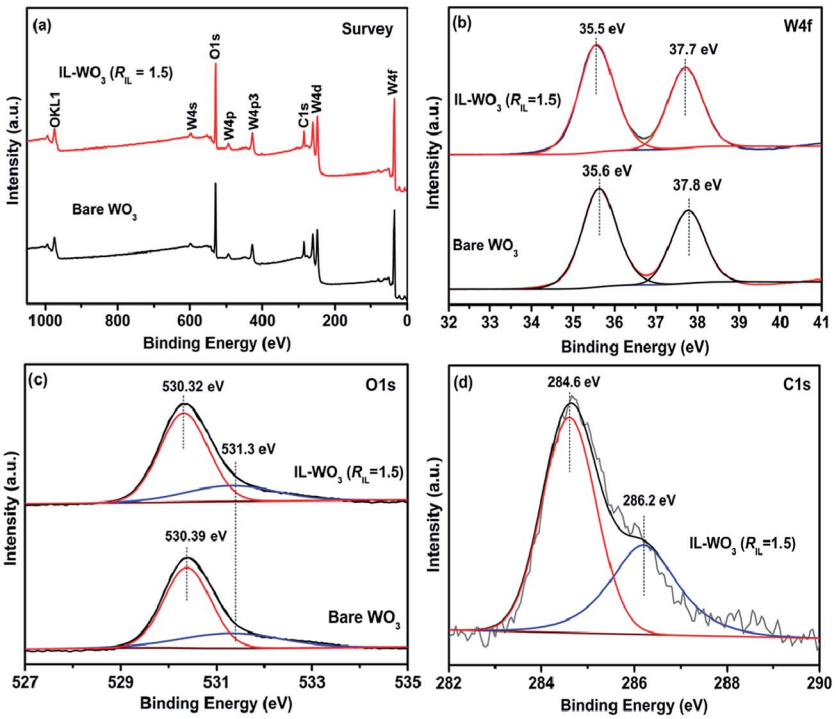

Fig. 4 XPS survey spectra of bare WO_3 and IL-WO_3 ($R_{IL} = 1.5$) (a). High-resolution XPS spectra of bare WO_3 and IL-WO_3 ($R_{IL} = 1.5$) in the regions of W4f (b), O1s (c) and C1s (d).

surface of WO_3.[34] According to the relative XPS areas, the atomic ratio of the surface oxygen (O_S) to the total oxygen ($O_L + O_S$) is reduced from 29.25% to 24.81% after the modification, indicating fewer surface hydroxyl groups on the IL-WO_3 than on the bare WO_3. Earlier investigations indicated that the surface modification of a semiconductor with ascorbic acid or ionic liquid caused a decrease in the number of surface hydroxyl groups.[21,22,35] The observed decrease in surface oxygen (O_S) could be because of the replacement of some surface hydroxyl groups by imidazolium after the modification. The peak in the C1s region of the IL-WO_3 can be deconvoluted into two contributions (Fig. 4d). They are attributed to the surface adventitious carbon (284.6 eV) and the carbon in the C–N groups of imidazolium (286.2 eV).[36,37] Therefore, the FT-IR and XPS studies allow us to conclude that the ionic liquid is bound to the surface of the WO_3 substrate.

The optical properties of these samples were investigated by UV-vis diffuse reflectance spectroscopy, as shown in Fig. 5. All the samples exhibited an intense absorption starting at approximately 475 nm, which corresponds to the band gap absorption of WO_3. In addition, UV-vis absorbance in the range of wavelengths shorter than 475 nm gradually increased with the increase in R_{IL} value. A similar phenomenon was also reported for [Bmim]I-modified BiOI.[22]

3.2. Photocatalytic behaviors

RhB is one of the representative organic dyes and has been widely used as a degradable target in the evaluation of photocatalytic activity.[38] To investigate the effects of the modification of [Bmim]I on the photocatalytic performance of WO_3, the photocatalytic activities of bare WO_3 and IL-WO_3 with different R_{IL} values were thus evaluated by observing the degradation of RhB under visible light irradiation ($\lambda > 420$), as shown in Fig. 6. It can be clearly observed that the self-degradation of RhB is negligible under visible light irradiation in the absence of catalyst. All the IL-WO_3 samples exhibit significantly higher photocatalytic activity than bare WO_3, demonstrating that the [Bmim]I modification is an effective method to enhance the photocatalysis of WO_3. The poor photocatalytic activity of the bare WO_3 can be attributed to a fast recombination of photogenerated electron–hole pairs because the multi-electron reduction of dioxygen is considerably less efficient than one-electron reduction of dioxygen, as mentioned above. The

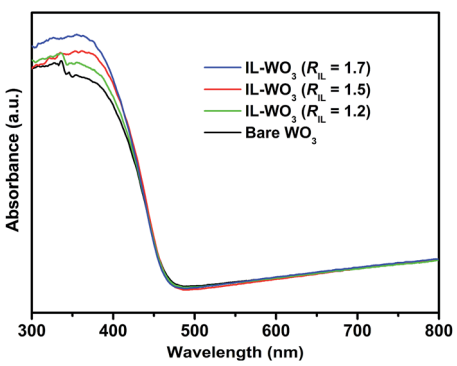

Fig. 5 UV-vis diffuse reflectance spectra of bare WO_3 and IL-WO_3 with different R_{IL} values.

Published on 04 August 2014. Downloaded by The University of Melbourne Libraries on 11/10/2014 09:08:59.

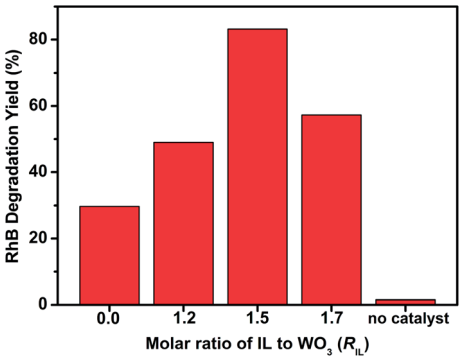

Fig. 6 Photocatalytic degradation yields of RhB over bare WO_3 and IL-WO_3 with different R_{IL} values under visible light irradiation ($\lambda > 420$) for 3 h.

highest RhB degradation yield occurred over the IL-WO_3 ($R_{IL} = 1.5$). Approximately 83% RhB degradation was achieved over this sample after visible light irradiation for 3 h compared to less than 30% RhB degradation over bare WO_3 within the same irradiation time. Moreover, the degradation yield of RhB over the IL-WO_3 ($R_{IL} = 1.7$) starts to decrease although it is still higher than that over bare WO_3. This may be due to the coverage of the WO_3 surface by excess [Bmim]I, leading to a decrease in surface active sites for RhB absorption.

Then, we investigated the effects of different scavengers on the degradation of RhB over bare WO_3 and IL-WO_3 ($R_{IL} = 1.5$) under visible light irradiation ($\lambda > 420$). As shown in Fig. 7, over both the samples, the degradation efficiency of RhB falls to almost half of the original with the addition of the $^{\bullet}OH$ scavenger TBA, and almost no degradation of RhB is observed when TEOA, an effective hole scavenger, is added to the photocatalytic reaction solution. These results reveal that both the photogenerated holes and $^{\bullet}OH$ radicals, as oxidation species, play equivalent roles in the degradation of RhB in both the systems. From the viewpoint of thermodynamics, the electron photoexcited on the conduction band of WO_3 (+0.3–0.5 V *vs.* NHE) is energetically capable of reducing oxygen molecules to form H_2O_2 through a two-electron reduction process [reaction 2, $E^{o}(O_2/H_2O_2) = +0.695$ V *vs.* NHE]. Thus, over both bare WO_3 and IL-WO_3, the $^{\bullet}OH$ radicals could be also produced through the reductive path of the conduction band electron (reaction 3) in addition to the direct reaction of the valence band holes with surface water or hydroxyl groups (reaction 4).

$$2e_{CB}^{-} + O_2 + 2H^{+} \rightarrow H_2O_2 \quad (2)$$

$$H_2O_2 + e_{CB}^{-} \rightarrow OH^{-} + {}^{\bullet}OH \quad (3)$$

$$h_{VB}^{+} + H_2O \text{ (or } -OH) \rightarrow {}^{\bullet}OH \quad (4)$$

Both $^{\bullet}OH$ radicals and holes photogenerated over WO_3 can degrade almost all the organic compounds due to their high redox potentials (+2.7 V and +3.1 V *vs.* NHE, respectively). Thus, no degradation of RhB occurring over both the samples in the presence of TEOA rules out the possibility of $^{\bullet}OH$ radical production through reaction 3. This implies that the photogenerated holes in both the samples are entirely responsible for both the direct degradation of RhB and the production of $^{\bullet}OH$ radicals (reaction 4), thus influencing the final photocatalytic properties. Based on the photocatalytic performances of bare WO_3 and IL-WO_3 in Fig. 6, it can be concluded that the production yield of photogenerated holes should be significantly higher over IL-WO_3 than over bare WO_3.

Furthermore, the photocatalytic stability and reusability of the IL-WO_3 catalyst was verified by performing the cyclic degradation process of fresh RhB solution with the used catalyst from the previous runs under the same conditions. As shown in Fig. 8, the IL-WO_3 ($R_{IL} = 1.5$) catalyst can be effectively recycled at least four times without an obvious decrease in its photocatalytic activity. This result suggests that the catalyst is sufficiently stable. In other words, the [Bmim]I is strongly bound to the surface of the WO_3 substrate and is not degraded during the photocatalytic degradation of pollutants, which is critical for practical applications.

3.3. Photogeneration of $^{\bullet}OH$ radicals

The hydroxyl radicals ($^{\bullet}OH$) formed in the visible light irradiated suspensions of bare WO_3 and IL-WO_3 ($R_{IL} = 1.5$) were detected by a fluorescence technique using terephthalic acid as

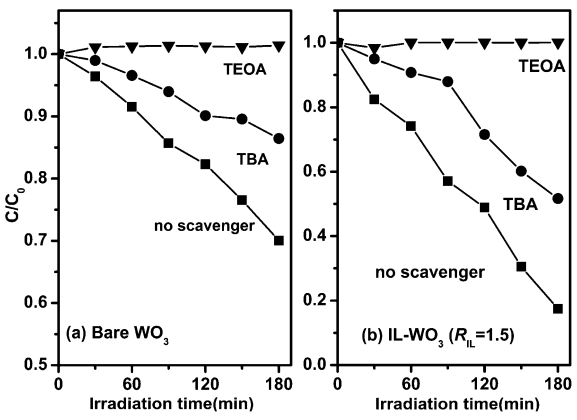

Fig. 7 Photocatalytic degradation of RhB over bare WO_3 and IL-WO_3 ($R_{IL} = 1.5$) in the presence and absence of different scavengers under visible light irradiation.

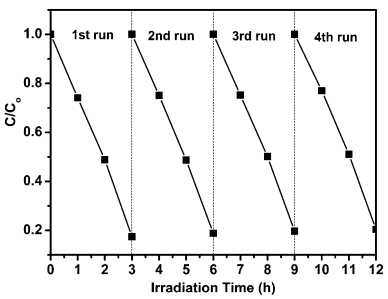

Fig. 8 Cyclic use of IL-WO_3 ($R_{IL} = 1.5$) for the photocatalytic degradation of RhB.

This journal is © The Royal Society of Chemistry 2014

Published on 04 August 2014. Downloaded by The University of Melbourne Libraries on 11/10/2014 09:08:59.

a chemical trap of ˙OH radicals, as shown in Fig. 9a and b. It can be observed that the fluorescence emission signals of 2-hydroxyterephthalic acid at approximately 425 nm can be observed for both the samples, suggesting the production of ˙OH radicals. The production of ˙OH radicals is considerably higher over IL-WO_3 (R_{IL} = 1.5) than over bare WO_3 within the same irradiation time. This result parallels the photocatalytic performances of the two samples shown in Fig. 6 and 7. It is shown in Fig. 7 that the production of ˙OH radicals over the two samples originates from the direct reaction of the valence band holes with surface water or hydroxyl groups (reaction 4) only. According to the characterization results mentioned above, the ionic liquid [Bmim]I is tightly bound to the surface of the WO_3, and no changes in the properties of the bulk WO_3 occur after the [Bmim]I modification. Moreover, the modification also causes an clear decrease in the number of surface hydroxyl groups, as confirmed by the XPS analysis above. As a result, it can be concluded that an efficient separation of the electron–hole pairs photoexcited over the WO_3 has been successfully achieved following surface modification with [Bmim]I.

It is well-known that the unique properties of [Bmim]I are largely related to the electronic structure of the aromatic cations (Scheme 1).[39] This electronic structure comprises a delocalized 3-center-4-electron configuration across the N1–C2–N3 moiety, a double bond between C4 and C5 at the opposite side of the ring, and a weak delocalization in the central region.[40] With this electronic structure, the surface-bound imidazolium ring can act as an electron-trapping group to stabilize an external electron through a conjugation effect.[41] In other words, because of the conjugation effect in the imidazolium ring, the [Bmim]I modification endows the surface of WO_3 with a stronger capability to stabilize the electron photoexcited at the conduction band. The electron stabilization on the surface-bound $[Bmim]^+$ retards the photoexcited electron transfer to the surface, probably forming H_2O_2 or H_2O through a multi-electron reduction process; however, the recombination of the photoexcited electron–hole pair is effectively suppressed. Consequently, more holes photoexcited over IL-WO_3 are allowed to react with surface water or hydroxyl groups to form hydroxyl radicals, or directly degrade the organic compound, which considerably enhances the photocatalytic efficiency.

To provide more convincing evidence for the capability of the surface-bound $[Bmim]^+$ as an electron-trapping group to inhibit the recombination of the electron–hole pairs photoexcited over IL-WO_3, we also detected the ˙OH radicals formed in visible light irradiated suspensions of bare WO_3 and IL-WO_3 (R_{IL} = 1.5) in the absence of soluble oxygen using the same procedure. According to the fluorescence emission spectra shown in Fig. 9c and d, the production of ˙OH radicals is negligible over bare WO_3 under visible light irradiation. This is because of a fast charge recombination in the absence of soluble oxygen as an electron scavenger. In the case of the IL-WO_3 (R_{IL} = 1.5), surprisingly, the number of ˙OH radicals apparently increases with the irradiation time. This indicates that the separation of the photoexcited electron–hole pairs can be still achieved over IL-WO_3 in the absence of soluble oxygen as an electron scavenger, allowing the holes to react with water or surface hydroxyl groups to form hydroxyl radicals. The charge separation occurring over IL-WO_3 in the absence of soluble oxygen is attributed to the electron-trapping effect of the surface-bound $[Bmim]^+$. The ˙OH radical measurements greatly clarify the electron-trapping capability of the imidazolium ring bound to the surface of WO_3, and greatly support the understanding of the mechanism of enhanced photocatalysis over IL-WO_3.

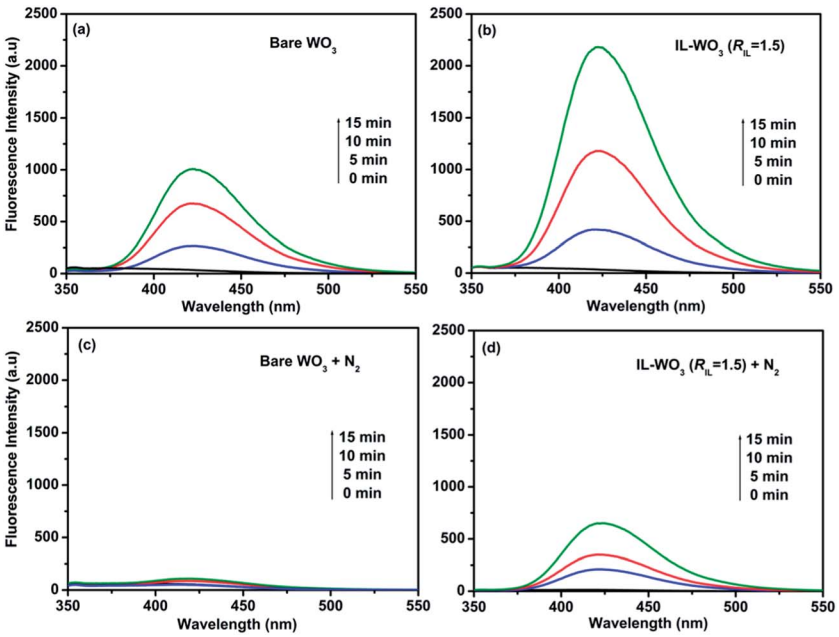

Fig. 9 Fluorescence emission intensities of the 2-hydroxyterephthalic acid produced in the visible light irradiated suspensions of bare WO_3 and IL-WO_3 (R_{IL} = 1.5) in the presence (a and b) and absence (b and d) of soluble oxygen.

Published on 04 August 2014. Downloaded by The University of Melbourne Libraries on 11/10/2014 09:08:59.

In summary, we demonstrated that the photocatalytic activity of WO_3 can be significantly enhanced by the surface modification of an ionic liquid [Bmim]I through a facile impregnation method. Various characterization results showed that the [Bmim]I is tightly bound to the surface of WO_3. It was revealed that the presence of the surface-bound $[Bmim]^+$ could effectively inhibit the recombination of photogenerated electron–hole pairs by trapping the electrons photoexcited on the conduction band, which is responsible for the observed enhancement of the photocatalysis. In addition, the [Bmim]I-modified WO_3 exhibits sufficient stability and long-lasting photocatalytic activity, which is beneficial for practical applications. We believe that this work could pave the way for the development of narrow band gap semiconductors with a deep valence band as efficient visible light photocatalytic materials.

Acknowledgements

This work was supported by National Natural Science Foundation of China (no. 21273281) and National Basic Research Program of China (973 Program, no. 2013CB632405).

References

1 X. C. Wang, K. Maeda, A. Thomas, K. Takanabe, G. Xin, J. M. Carlsson, K. Domen and M. Antonietti, *Nat. Mater.*, 2009, **8**, 76–80.
2 H.-Y. Jiang, J. Liu, K. Cheng, W. Sun and J. Lin, *J. Phys. Chem. C*, 2013, **117**, 20029–20036.
3 J. Low, J. Yu, Q. Li and B. Cheng, *Phys. Chem. Chem. Phys.*, 2014, **16**, 1111–1120.
4 C. Santato, M. Ulmann and J. Augustynski, *Adv. Mater.*, 2001, **13**, 511–514.
5 M. Sadakane, K. Sakaki, H. Kunioku, B. Ohtani, W. Ueda and R. Abe, *Chem. Commun.*, 2008, 6552–6554.
6 G. R. Bamwenda, T. Uesigi, Y. Abe, K. Sayama and H. Arakawa, *Appl. Catal., A*, 2001, **205**, 117–128.
7 W. Morales, M. Cason, O. Aina, N. R. de Tacconi and K. Rajeshwar, *J. Am. Chem. Soc.*, 2008, **130**, 6318–6319.
8 J. Yu, L. Qi, B. Cheng and X. Zhao, *J. Hazard. Mater.*, 2008, **160**, 621–628.
9 R. Abe, H. Takami, N. Murakami and B. Ohtani, *J. Am. Chem. Soc.*, 2008, **130**, 7780–7781.
10 J. Kim, C. W. Lee and W. Choi, *Environ. Sci. Technol.*, 2010, **44**, 6849–6854.
11 Z.-G. Zhao and M. Miyauchi, *Angew. Chem., Int. Ed.*, 2008, **47**, 7051–7055.
12 T. Arai, M. Horiguchi, M. Yanagida, T. Gunji, H. Sugihara and K. Sayama, *Chem. Commun.*, 2008, 5565–5567.
13 A. Tanaka, K. Hashimoto and H. Kominami, *J. Am. Chem. Soc.*, 2014, **136**, 586–589.
14 T. Arai, M. Horiguchi, M. Yanagida, T. Gunji, H. Sugihara and K. Sayama, *J. Phys. Chem. C*, 2009, **113**, 6602–6609.
15 Y. Nosaka, S. Takashi, H. Sakamoto and A. Y. Nosaka, *J. Phys. Chem. C*, 2011, **115**, 21283–21290.
16 X. An, J. C. Yu, Y. Wang, Y. Hu, X. Yu and G. Zhang, *J. Mater. Chem.*, 2012, **22**, 8525–8531.
17 Z.-G. Zhao and M. Miyauchi, *J. Phys. Chem. C*, 2009, **113**, 6539–6546.
18 T. Welton, *Chem. Rev.*, 1999, **99**, 2071–2083.
19 R. Katoh, M. Hara and S. Tsuzuki, *J. Phys. Chem. B*, 2008, **112**, 15426.
20 X. Meng and F.-S. Xiao, *Chem. Rev.*, 2014, **114**, 1521–1543.
21 S. Hu, A. Wang, X. Li, Y. Wang and H. Löwe, *Chem.–Asian J.*, 2010, **5**, 1171–1177.
22 Y. Wang, K. Deng and L. Zhang, *J. Phys. Chem. C*, 2011, **115**, 14300–14308.
23 G. V. Buxton, C. L. Greenstock, W. P. Helman and A. B. Ross, *J. Phys. Chem. Ref. Data*, 1988, **17**, 513–886.
24 K. Ishibashi, A. Fujishima, T. Watanabe and K. Hashimoto, *Electrochem. Commun.*, 2000, **2**, 207–210.
25 M. Breedon, P. Spizzirri, M. Taylor, J. du Plessis, D. McCulloch, J. Zhu, L. Yu, Z. Hu, C. Rix, W. Wlodariski and K. Kalantarzadeh, *Cryst. Growth Des.*, 2010, **10**, 430–439.
26 A. Baserga, V. Russo, F. Difonzo, A. Bailini, D. Cattaneo, C. Casari, A. Libassi and C. Bottani, *Thin Solid Films*, 2007, **515**, 6465–6469.
27 B. Fitchett and J. C. Conboy, *J. Phys. Chem. B*, 2004, **108**, 20225–20262.
28 T. Wang, H. Kaper, M. Antonietti and B. Smarsly, *Langmuir*, 2007, **23**, 1489–1495.
29 R. J. Colton and J. W. Rabalais, *Inorg. Chem.*, 1976, **15**, 236–238.
30 Y. Baek and K. Yong, *J. Phys. Chem. C*, 2007, **111**, 1213–1218.
31 J. N. Yao, P. Chen and A. Fujishima, *Electroanal. Chem.*, 1996, **406**, 223–226.
32 S. B. Bon, L. Valentini, R. Verdejo, J. L. G. Fierro, L. Peponi, M. A. Lopez-Manchada and J. M. Kenny, *Chem. Mater.*, 2009, **21**, 3433–3438.
33 J. Qin, M. Cao, N. Li and C. Hu, *J. Mater. Chem.*, 2011, **21**, 17167–17174.
34 Y. W. Wang, Y. Huang, W. K. Ho, L. Z. Zhang, Z. G. Zou and S. C. Lee, *J. Hazard. Mater.*, 2009, **169**, 77–87.
35 Y. Ou, J. D. Lin, H. M. Zou and D. W. Liao, *J. Mol. Catal. A: Chem.*, 2005, **241**, 59–64.
36 S. Biniak, G. Szymanski, J. Siedlewski and A. Swiatkowski, *Carbon*, 1997, **35**, 1799–1810.
37 X. Tang, Y. Li, X. Huang, Y. Xu, H. Zhu, J. Wang and W. Shen, *Appl. Catal., B*, 2006, **62**, 265–273.
38 J. S. Chen, J. Liu, S. Z. Qiao, R. Xu and X. W. Lou, *Chem. Commun.*, 2011, **47**, 10443–10445.
39 H. Weingartner, *Angew. Chem., Int. Ed.*, 2008, **47**, 654–670.
40 P. A. Hunt, B. Kirchmer and T. Welton, *Chem.–Eur. J.*, 2006, **12**, 6762–6775.
41 R. T. Morrison and R. N. Boyd, *Organic Chemistry*, Allyn and Bacon, London, 4th edn, 1983.

 This journal is © The Royal Society of Chemistry 2014